

Stationarity Test for Wireless Communication Channels

Dmitry Umansky
Faculty of Engineering and Science
University of Agder
Service Box 509, N-4898, Grimstad, Norway
Email: dmitry.umansky@uia.no

Matthias Pätzold
Faculty of Engineering and Science
University of Agder
Service Box 509, N-4898, Grimstad, Norway
Email: matthias.paetzold@uia.no

Abstract—In this article, we propose a new test to determine the intervals of stationarity for wireless communication channels. The intervals of stationarity are identified by comparing the delay power spectral density (PSD) estimated at different time instances. The performance of the proposed stationarity test has been evaluated based on the synthetic data generated using a channel simulator. The analysis of the stationarity intervals for two radio communication channels measured in different propagation scenarios reveals that the number and the length of the stationarity intervals decrease as the dimensions of the channel matrix increase.

I. INTRODUCTION

A random linear time-variant channel model based on the wide-sense stationarity uncorrelated scattering (WSSUS) assumption was introduced in [1]. In the same work, the author pointed out that real-world radio channels often demonstrate ‘quasi-stationary’ behavior, i.e., the WSSUS assumption can be accepted only for limited intervals of time and frequency. Consequently, it is of great interest to develop test procedures that can be used to reliably identify such regions of stationarity for wireless channels.

A number of stationarity tests have been proposed in the literature related to such disciplines as wireless channel modeling, spectrum analysis, signal detection, etc. The correlation between consecutive ‘instantaneous’ delay PSDs has been used in [2] to identify the local region of stationarity (LRS) for wireless channels. A nonstationarity detector based on the time-variant autoregressive (TVAR) model has been described in [3]. In [4], the authors suggest to identify the intervals of stationarity by analyzing changes in the wave-number spectrum estimated at different locations. The use of the nonparametric *run*-test [5] for determining the stationarity intervals of radio channels has been investigated in [6]. An interesting test for wide-sense stationarity of multiple-input multiple-output (MIMO) wireless channels has been developed in [7]. This approach is based on analyzing the evolutionary spectrum of a signal estimated at different instances of time [8].

In this paper, we propose a new statistical test for determining the time intervals of stationarity for wireless communication channels. In the development of the test the primary importance has been assigned to analyzing the stationarity of radio channels without time averaging. This approach allows

to skip windowing of the measurement data in time, which is often (if not always) has to be done heuristically. Hence, a greater level of automation in the test procedure can be provided. The proposed test is based on the hypothesis that the estimated delay PSD of a channel does not change with time over the interval of stationarity. The test is applicable both to single-input single-output (SISO) and MIMO radio channels. The design of the test procedure described in Section II relies on the definition of a random (multivariate) WSS process (see, e.g. [9]). In particular, we assume that the time-variant frequency response (TVFR) of a channel is a random Gaussian process, WSS (jointly WSS, for MIMO channels) with respect to (w.r.t.) frequency. However, it appears that this assumption is not restrictive, if, similar to [2], the channel stationarity intervals are defined as the intervals over which the locations of the scatterers, transmitter, and receiver do not change significantly.

The rest of the paper is organized as follow. In Section II, the stationarity test for SISO and MIMO wireless communication channels is developed. The results of the performance evaluation for the proposed test are presented in Section III. The analysis of the stationarity intervals for two different real-world propagation environments is presented in Section IV. The concluding remarks are given in Section V.

II. STATIONARITY TEST

Let the TVFR $H(f', t)$ describing a SISO wireless channel in frequency f' and time t be a complex two-dimensional (2D) Gaussian random process. We assume that the TVFR $H(f', t)$ is a WSS process w.r.t. frequency f' . This assumption together with the presumed Gaussianity of the 2D random process $H(f', t)$ allows us to consider the measured TVFR as an autocorrelation-ergodic process w.r.t. frequency [5]. Hence, it is legitimate to estimate the correlation characteristics of the TVFR at the time t_n by averaging over frequency.

Wide-sense stationarity of the TVFR $H(f', t)$ w.r.t. time implies that the delay PSD is time-invariant. This observation forms the basics of the statistical test proposed for validating the hypothesis that the measured TVFR $H(f', t)$ is a WSS processes w.r.t. time.

In the following subsection, we describe the stationarity test for SISO wireless channels. In Subsection II-B, the procedure

will be extended to test the stationarity of MIMO radio channels.

A. SISO Channels

Suppose that the TVFR $H(f', t)$ of a SISO radio channel has been measured at discrete frequencies $f'_m = -B/2 + m\Delta f' \in [-B/2, B/2]$, $m = 0, \dots, M-1$, and at discrete time instances $t_n = n\Delta t \in [0, T]$, $n = 0, \dots, N-1$. The frequency bandwidth and the measurement time interval are denoted as B and T , respectively. We can represent the measured TVFR of the channel in a matrix form

$$\mathbf{H} = \begin{pmatrix} H[0, 0] & \dots & H[0, N-1] \\ \vdots & \ddots & \vdots \\ H[M-1, 0] & \dots & H[M-1, N-1] \end{pmatrix}. \quad (1)$$

The elements $H[m, n]$ of the matrix (1) are complex Gaussian random variables. As it was mentioned above, we assume that the columns of the channel matrix \mathbf{H} , i.e., the snapshots of the channel's TVFR at time instances t_n , are ergodic processes. Thus, for each of these processes, we can determine the mean

$$\eta[n] = \langle H[m, n] \rangle_{f'} \quad (2)$$

and the frequency autocorrelation function (FACF)

$$r_{f'}[\kappa, n] = \langle H[m, n]H^*[m + \kappa, n] \rangle_{f'} \quad (3)$$

where $*$ designates the complex conjugate and $\langle \cdot \rangle_{f'} = \frac{1}{M} \sum_{m=0}^{M-1} (\cdot)$ denotes averaging over frequency.

The delay PSD of the radio channel at time t_n is given by

$$P(\tau', t_n) = \Delta f' \sum_{\kappa=-\infty}^{\infty} r_{f'}[\kappa, n] e^{j2\pi\tau'\kappa\Delta f'}. \quad (4)$$

where τ' stands for the propagation delay.

According to the definition, wide-sense stationarity of the TVFR \mathbf{H} w.r.t. time requires that the mean $\eta[n]$ and the FACF $r_{f'}[\kappa, n]$ are time-invariant, i.e.,

$$\eta[n] = \eta \quad (5)$$

$$r_{f'}[\kappa, n] = r_{f'}[\kappa]. \quad (6)$$

Condition (6) corresponds to the time-invariance of the delay PSD $P(\tau', t_n)$, which can be written as

$$P(\tau', t_{n_1}) = P(\tau'). \quad (7)$$

Using (7), we can formulate the null hypothesis \mathcal{H}_0 as follows

$$\mathcal{H}_0 : (P(\tau', t_{n_1}) - P(\tau', t_{n_2})) = 0, \quad t_{n_1} \neq t_{n_2} \quad (8)$$

which implies that the delay PSD at time t_{n_1} equals the delay PSD at time t_{n_2} .

Note that the hypothesis \mathcal{H}_0 also suggests the equality of the mean values, i.e., $\eta[n_1] = \eta[n_2]$. This follows from the observation that

$$\int_{-\infty}^{\infty} P(\tau', t_n) d\tau' = r_{f'}[0, n] = \sigma^2[n] + \eta^2[n] \quad (9)$$

where the variance $\sigma^2[n] = \langle (H[m, n] - \eta_H[n])(H[m, n] - \eta_H[n])^* \rangle_{f'}$.

The procedure presented below allows us to compare the delay PSDs estimated at two different time instances¹ and determine whether the hypothesis \mathcal{H}_0 can be exceeded.

The following five-step data processing algorithm significantly simplifies the statistical analysis of the null hypothesis \mathcal{H}_0 .

Step 1. The n -th column of the channel matrix \mathbf{H} in (1) is divided into K nonoverlapping segments each of length M_s . Let

$$x_m^{(k)} = H[(k-1)M_s + m, n], \quad m = 0, \dots, M_s - 1 \quad (10)$$

denote a complex data sequence corresponding to the k -th segment, $k = 1, \dots, K$.

Step 2. For each of the K sequences $\{x_m^{(k)}\}_{m=0}^{M_s-1}$, $k = 1, \dots, K$, calculate the periodogram at the discrete delays $\tau'_q = \frac{q}{M_s\Delta f'}$, $q = 0, \dots, M_s - 1$,

$$\hat{P}_q^{(k)} = \frac{\Delta f'}{M_s} \left| \sum_{m=0}^{M_s-1} x_m^{(k)} e^{j2\pi\tau'_q\Delta f'm} \right|^2. \quad (11)$$

It is known (see, e.g., [10]) that asymptotically ($M_s \rightarrow \infty$)

$$\hat{P}_q^{(k)} \sim \begin{cases} P_q \chi_2^2/2, & q = 1, \dots, \frac{M_s}{2} - 1, \frac{M_s}{2} + 1, \dots, M_s - 1 \\ P_q \chi_1^2, & q = 0 \text{ and } \frac{M_s}{2} \end{cases} \quad (12)$$

where χ_1^2 and χ_2^2 signify the chi-square distributions with one and two degrees of freedom, respectively. The sequence $\{P_q\}_{q=0}^{M_s-1}$ denotes the delay PSD at the discrete delays $\{\tau'_q\}$.

Step 3. For each of the K periodograms $\{\hat{P}_q^{(k)}\}_{q=0}^{M_s-1}$, $k = 1, \dots, K$, create an auxiliary data sequence $\{y_p^{(k)}\}_{p=0}^{2M_s-3}$ as follows

$$y_p^{(k)} = \begin{cases} \hat{P}_p^{(k)}, & p = 0, \dots, M_s - 1 \\ \hat{P}_{2M_s-2-p}^{(k)}, & p = M_s, \dots, 2M_s - 3. \end{cases} \quad (13)$$

Step 4. For each of the K sequences $\{y_p^{(k)}\}_{p=0}^{2M_s-3}$, $k = 1, \dots, K$, estimate the cepstrum $\hat{\Phi}_l^{(k)}$ at the discrete frequencies $\omega_l = l\pi/(M_s - 1)$, $l = 0, \dots, 2M_s - 3$,

$$\hat{\Phi}_l^{(k)} = \frac{1}{2M_s - 2} \sum_{p=0}^{2M_s-3} \ln(y_p^{(k)}) e^{-j\omega_l p}. \quad (14)$$

Here, we implicitly assume that $y_p^{(k)} > 0$ for all p , which is true in practical situations. Also note that due to the symmetry in $\{y_p^{(k)}\}_{p=0}^{2M_s-3}$, $\hat{\Phi}_l^{(k)}$ is real and $\hat{\Phi}_{2M_s-2-l}^{(k)} = \hat{\Phi}_l^{(k)}$ for $l = 0, \dots, M_s - 1$.

It has been shown in [11] that asymptotically, i.e., as $M_s \rightarrow \infty$, the estimated cepstrum $\{\hat{\Phi}_l^{(k)}\}_{l=0}^{M_s-1}$ follows the multivariate Gaussian distribution with the covariance matrix \mathbf{C} . The matrix \mathbf{C} is a constant diagonal matrix independent of the periodogram $\{\hat{P}_q^{(k)}\}_{q=0}^{M_s-1}$.

¹As will be shown shortly, the comparison is actually done in terms of the estimated cepstrum. Recall that the cepstrum of a signal is related to the PSD through an invertible one-to-one transformation.

Step 5. Stack the estimated cepstrum sequences $\{\hat{\Phi}_l^{(k)}\}_{l=0}^{M_s-1}$, $k = 1, \dots, K$, as columns into a matrix \mathbf{U}_n of dimensions $M_s \times K$. Let the column vector $\bar{\mathbf{u}}_n$ of dimensions $M_s \times 1$ contain the sample mean of each row of the matrix \mathbf{U}_n .

To verify the hypothesis \mathcal{H}_0 , we apply the algorithm described above to the n_1 -th and the n_2 -th columns of the channel matrix \mathbf{H} representing the channel frequency response at two distinct time instances t_{n_1} and t_{n_2} . As the outcome, we obtain two matrices \mathbf{U}_{n_1} , \mathbf{U}_{n_2} and two column vectors $\bar{\mathbf{u}}_{n_1}$, $\bar{\mathbf{u}}_{n_2}$. The vectors $\bar{\mathbf{u}}_{n_1}$ and $\bar{\mathbf{u}}_{n_2}$ are the cepstrum estimates at the time instances t_{n_1} and t_{n_2} , respectively. The matrices \mathbf{U}_{n_1} , \mathbf{U}_{n_2} and the vectors $\bar{\mathbf{u}}_{n_1}$, $\bar{\mathbf{u}}_{n_2}$ can now be supplied to the Hotelling's T^2 -test [12], [13].

We first define two matrices

$$\begin{aligned} \mathbf{S}_1 &= \mathbf{U}_{n_1} \mathbf{U}_{n_1}^T - K \bar{\mathbf{u}}_{n_1} \bar{\mathbf{u}}_{n_1}^T \\ \mathbf{S}_2 &= \mathbf{U}_{n_2} \mathbf{U}_{n_2}^T - K \bar{\mathbf{u}}_{n_2} \bar{\mathbf{u}}_{n_2}^T \end{aligned} \quad (15)$$

where K is the number of segments (see *Step 1* of the algorithm above) and the operator $\{\cdot\}^T$ denotes transposition. It is known [12] that the statistic $\varphi(\mathbf{S}_1, \mathbf{S}_2, \bar{\mathbf{u}}_{n_1}, \bar{\mathbf{u}}_{n_2})$ given by

$$\begin{aligned} \varphi(\mathbf{S}_1, \mathbf{S}_2, \bar{\mathbf{u}}_{n_1}, \bar{\mathbf{u}}_{n_2}) &= \\ &= \frac{K(2K - M_s - 1)}{2M_s} (\bar{\mathbf{u}}_{n_1} - \bar{\mathbf{u}}_{n_2})^T (\mathbf{S}_1 + \mathbf{S}_2)^{-1} (\bar{\mathbf{u}}_{n_1} - \bar{\mathbf{u}}_{n_2}) \end{aligned} \quad (16)$$

follows the F-distribution, i.e., $\varphi(\mathbf{S}_1, \mathbf{S}_2, \bar{\mathbf{u}}_{n_1}, \bar{\mathbf{u}}_{n_2}) \sim F(M_s, 2K - M_s - 1)$.

Thus, the null hypothesis \mathcal{H}_0 in (8) is accepted if

$$\varphi(\mathbf{S}_1, \mathbf{S}_2, \bar{\mathbf{u}}_{n_1}, \bar{\mathbf{u}}_{n_2}) < f_\alpha \quad (17)$$

where f_α is the critical value corresponding to the $100(1-\alpha)\%$ confidence level.

B. MIMO Channels

Let us consider a MIMO wireless channel with N_T transmitting and N_R receiving antennas. Each of the $N_T N_R$ subchannels, i.e., communication links between each transmitting and each receiving antennas, is represented by the measured TVFR channel matrix \mathbf{H}_i , $i = 1, \dots, N_T N_R$, defined in (1). As in the previous subsection, we assume that the elements $H_i[m, n]$ of the channel matrices \mathbf{H}_i are complex Gaussian random variables. Furthermore, it is assumed that at every time instance t_n the TVFRs of all the subchannels are jointly WSS processes with respect to frequency.

The delay cross power spectral densities (CPSDs) at time t_n can be defined as

$$\begin{aligned} P_{H_i, H_{i'}}(\tau', t_n) &= \Delta f' \sum_{\kappa=-\infty}^{\infty} r_{f'_{H_i, H_{i'}}}[\kappa, n] e^{j2\pi\tau'\kappa\Delta f'}, \\ & i, i' = 1, \dots, N_T N_R \end{aligned} \quad (18)$$

where $r_{f'_{H_i, H_{i'}}}[\kappa, n]$ is the frequency cross correlation function (FCCF) at time t_n between the TVFR \mathbf{H}_i of the i -th

subchannel and the TVFR $\mathbf{H}_{i'}$ of the i' -th subchannel given by

$$\begin{aligned} r_{f'_{H_i, H_{i'}}}[\kappa, n] &= \langle H_i[m, n] H_{i'}^*[m + \kappa, n] \rangle_{f'}, \\ & i, i' = 1, \dots, N_T N_R. \end{aligned} \quad (19)$$

The wide-sense stationarity of the considered MIMO channel w.r.t. time requires that the delay CPSDs $P_{H_i, H_{i'}}(\tau', t_n)$, $i, i' = 1, \dots, N_T N_R$, are time invariant. Therefore, we can express the null hypothesis \mathcal{H}_0 as

$$\begin{aligned} \mathcal{H}_0 : & (P_{H_i, H_{i'}}(\tau', t_{n_1}) - P_{H_i, H_{i'}}(\tau', t_{n_2})) = 0, \\ & i, i' = 1, \dots, N_T N_R \text{ and } t_{n_1} \neq t_{n_2}. \end{aligned} \quad (20)$$

Our objective here is to validate the null hypothesis \mathcal{H}_0 by using the procedure developed in the previous subsection for SISO wireless channels.

In [14, Chapter 15], the author describes an interesting approach to estimating CPSDs. It is mentioned, however, that this approach cannot guarantee the magnitude squared coherence [14] between two subchannels to be always bounded by 1. As we are interested in the time variation of the estimated delay CPSD and not in the estimated coherence between the channels, this drawback is not relevant for our purpose.

Following [14], the real and the imaginary parts of the delay CPSDs $P_{H_i, H_{i'}}(\tau', t_n)$ can be written as

$$\begin{aligned} \Re\{P_{H_i, H_{i'}}(\tau', t_n)\} &= \frac{1}{2} (P_{Z_{ii'}, Z_{ii'}}(\tau', t_n) - P_{H_i, H_i}(\tau', t_n) - P_{H_{i'}, H_{i'}}(\tau', t_n)) \\ \Im\{P_{H_i, H_{i'}}(\tau', t_n)\} &= \frac{1}{2} (P_{W_{ii'}, W_{ii'}}(\tau', t_n) - P_{H_i, H_i}(\tau', t_n) - P_{H_{i'}, H_{i'}}(\tau', t_n)) \end{aligned} \quad (21)$$

for $i, i' = 1, \dots, N_T N_R$ and $i \neq i'$, where $P_{Z_{ii'}, Z_{ii'}}(\tau', t_n)$ and $P_{W_{ii'}, W_{ii'}}(\tau', t_n)$ denote, respectively, the delay PSDs of the signals

$$\begin{aligned} Z_{ii'}[m, n] &= H_i[m, n] + H_{i'}[m, n] \\ W_{ii'}[m, n] &= H_i[m, n] + jH_{i'}[m, n]. \end{aligned} \quad (22)$$

Taking (21) into account, the null hypothesis \mathcal{H}_0 in (20) can be reformulated as follows

$$\begin{aligned} \mathcal{H}_{0a} : & (P_{H_i, H_i}(\tau', t_{n_1}) - P_{H_i, H_i}(\tau', t_{n_2})) = 0, \\ & i = 1, \dots, N_T N_R \text{ and } t_{n_1} \neq t_{n_2} \\ \mathcal{H}_{0b} : & (P_{Z_{ii'}, Z_{ii'}}(\tau', t_{n_1}) - P_{Z_{ii'}, Z_{ii'}}(\tau', t_{n_2})) = 0, \\ & i, i' = 1, \dots, N_T N_R, i \neq i' \text{ and } t_{n_1} \neq t_{n_2} \\ \mathcal{H}_{0c} : & (P_{W_{ii'}, W_{ii'}}(\tau', t_{n_1}) - P_{W_{ii'}, W_{ii'}}(\tau', t_{n_2})) = 0, \\ & i, i' = 1, \dots, N_T N_R, i \neq i' \text{ and } t_{n_1} \neq t_{n_2}. \end{aligned} \quad (23)$$

Note the absence of the delay CPSDs in (23). Thus the null hypotheses $\{\{\mathcal{H}_{0a}\}, \{\mathcal{H}_{0b}\}, \{\mathcal{H}_{0c}\}\}$ can be verified by using the method described in Subsection II-A for SISO channels.

The total number of the null hypotheses in (23) is equal to $(N_T N_R)^2$. Based on the results of testing these hypotheses, the decision is to be taken on whether a MIMO channel

is WSS. One approach is to accept the wide-sense stationarity of a MIMO channel only if all of the hypotheses $\{\{\mathcal{H}_{0a}\}, \{\mathcal{H}_{0b}\}, \{\mathcal{H}_{0c}\}\}$ have been validated. The probability of the Type I error, i.e., erroneously rejecting any of the hypotheses $\{\{\mathcal{H}_{0a}\}, \{\mathcal{H}_{0b}\}, \{\mathcal{H}_{0c}\}\}$, is equal to α (see (17)). Thus, assuming the independence of such errors, the probability of falsely rejecting the hypothesis that a MIMO channel is WSS can be expressed as

$$\Pr\{\text{error}\} = 1 - (1 - \alpha)^{(N_T N_R)^2}. \quad (24)$$

As it follows from Table I, even for MIMO channels of

TABLE I
PROBABILITY $\Pr\{\text{ERROR}\}$ OF WRONG REJECTION OF THE HYPOTHESIS THAT A MIMO CHANNEL OF DIMENSIONS $N_T \times N_R$ IS WSS

$N_T \times N_R$	$\alpha = 0,05$	$\alpha = 0,01$	$\alpha = 0,003$
2×2	0.36	0.14	0.047
3×3	0.984	0.557	0.216
4×4	0.9998	0.924	0.537

moderate dimensions, the probability of error $\Pr\{\text{error}\}$ is unacceptable. A possible solution to this problem is to allow a certain number of hypotheses in (23) to be rejected. For example, suppose we verify the stationarity of a MIMO 2×2 channel. The probability of error in a single hypothesis test α is set to 0.01. Our goal is to maintain $\Pr\{\text{error}\}$ equal to or less than α for the decision based on the results of $(N_T N_R)^2 = 16$ hypothesis tests. Using the Bernoulli trials scheme [9], it can be easily shown that in this case $\Pr\{\text{error}\} \leq 0.01$ if at least 1 of 16 hypotheses in (23) is allowed to be rejected.

Let us now reconsider the assumption of the wide-sense stationarity of the channel TVFR w.r.t. frequency. What can be said if this assumption is not valid? As it is described in Subsection II-A, the Hotelling's T^2 -test verifies the hypothesis that the two column vectors $\bar{\mathbf{u}}_{n_1}$ and $\bar{\mathbf{u}}_{n_2}$ are equal. If the WSS assumption of the TVFR in the frequency domain is not valid, then the vectors $\bar{\mathbf{u}}_{n_1}$ and $\bar{\mathbf{u}}_{n_2}$ are derived from the inconsistent estimates of the delay PSDs. Thus, the null hypotheses formulated in (8) and (23) cannot be verified, i.e., nothing can be said about WSS property of the channel TVFR w.r.t. time.

However, it is plausible to assume that if the geographical locations of the scatterers, transmitter, and receiver remain unchanged between the time instances t_{n_1} and t_{n_2} , then the vectors $\bar{\mathbf{u}}_{n_1}$ and $\bar{\mathbf{u}}_{n_2}$ are equal. In this case, the tests developed above verify the empirical channel stationarity as defined in [2].

III. PERFORMANCE EVALUATION

We have evaluated the performance of the proposed stationarity test on synthetic TVFRs generated using the geometrical two-ring channel simulation model (see e.g., [15]). Some of the channel simulator parameters are specified below

- Carrier frequency: 5.255 GHz;
- Bandwidth: $B = 100$ MHz;
- Receiving antenna: uniform linear array;

- Transmitting antenna: uniform linear array;
- Antenna element spacing at the receiver: 0.5λ ;
- Antenna element spacing at the transmitter: 0.5λ ;
- Interval between the frequencies: $\Delta f' = 1.957 \cdot 10^5$ Hz;
- Time between channel snapshots: $\Delta t = 0.02$ s;
- Maximum Doppler frequency: 22 Hz;
- SNR: 10 dB.

A hundred scatterers are located on the rings around the base station and the mobile station [15]. It has been verified that the Doppler frequencies and the propagation delays are different for all propagation paths. Under this condition the generated TVFR is ergodic w.r.t. time and frequency [16]. All the propagation path gains are equal to $1/\sqrt{100}$. The parameters of the channel simulator do not change with time. It has been observed that for the confidence level of 99% ($\alpha = 0.01$) and the parameter $M_s = 16$, the error probability $\Pr\{\text{error}\}$ is equal to 0.0073, 0.0145, and 0.0064 for SISO, 2×2 MIMO, and 4×4 MIMO channels, respectively.

IV. APPLICATIONS TO MEASUREMENT DATA

In this section, we present the results of applying the test procedure developed in Section II to real-world measurement data. The measurement campaign has been conducted by Telenor R&D, Norway.

The first propagation environment corresponds to an urban micro-cell site with a regular street grid. The building mass is homogenous. The materials used are mostly brick and concrete. The building height varies from 20–30 m. The transmitting antenna is positioned at 1.5 m above the ground on a mobile trolley. The trolley moves with the walking speed. The stationary receiving antenna is mounted at 1.8 m height above the ground. The measurements have been obtained by using a wideband channel sounder with synchronized multiplexing between transmitter and receiver. A linear frequency chirp signal is used for channel sounding. Additionally, the following parameters are specified:

- Carrier frequency: 5.255 GHz;
- Bandwidth: $B = 100$ MHz;
- Receiving antenna: 8 element uniform linear array;
- Transmitting antenna: 8 element uniform linear array;
- Antenna element spacing at the receiver: 0.5λ ;
- Antenna element spacing at the transmitter: 0.5λ ;
- Interval between the frequencies: $\Delta f' = 1.957 \cdot 10^5$ Hz;
- Time between channel snapshots: $\Delta t = 0.07$ s;
- Impulse response length: 5.12 μ s.

A series of the measured impulse responses for this propagation scenario is shown in Fig. 1. The time variation of the mean-square value of the TVFR can be observed in Fig. 2. The antenna arrays at the transmitter and the receiver allow us to investigate the distribution of the stationarity interval lengths for SISO and MIMO channels. The stationarity intervals have been determined by using the test described in Section II. The parameter M_s (see Subsection II-A) is equal to 16. The confidence level is set to 99% ($\alpha = 0.01$).

The complementary cumulative distribution functions (CCDFs) of the length of the stationarity intervals obtained for

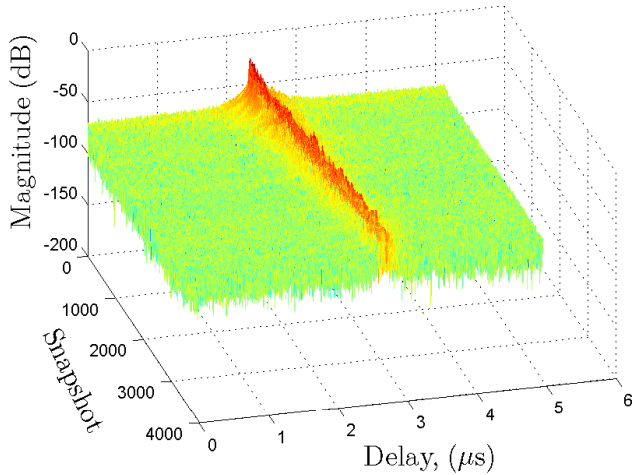


Fig. 1. Magnitude of the impulse response. Urban micro-cell site with a regular street grid.

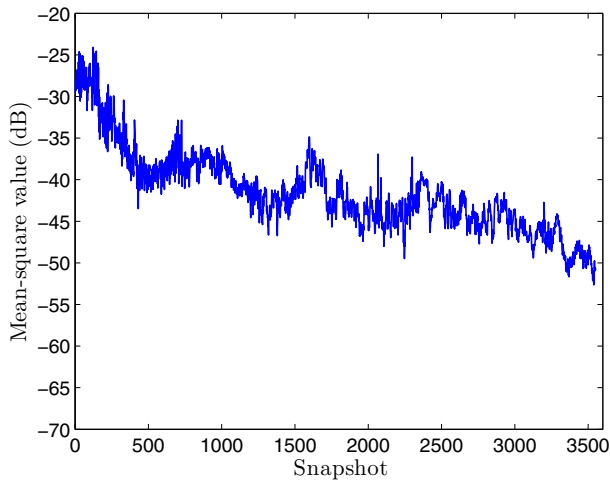


Fig. 2. Mean-square value of the TVFR. Urban micro-cell site with a regular street grid.

SISO, 2×2 MIMO, and 4×4 MIMO channels are presented in Fig. 3. The mean length of the identified stationarity intervals decreases from 0.59 s for the SISO channel to 0.28 s for the 2×2 MIMO and 0.18 s for 4×4 MIMO channels². The standard deviations of the stationarity interval lengths are equal to 0.79 s, 0.34 s, and 0.21 s, for the SISO, 2×2 MIMO, and 4×4 MIMO channels, respectively. As can be seen from Fig. 3, the percentage of the identified stationarity intervals longer than or equal to for example 0.5 s drops from 40% for the SISO channel to 20% for the 2×2 MIMO and 10% s for 4×4 MIMO channels. Similar observations have been reported in [7], where the stationarity intervals for SISO and 2×2 MIMO channels have been compared.

²Since the moving speed is known only approximately, the stationarity intervals are measured in seconds and not in wavelengths, which otherwise might be a preferable measure.

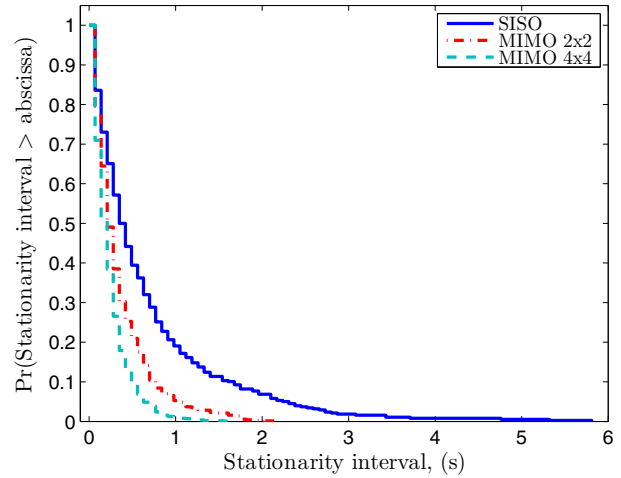


Fig. 3. CCDF of the length of the stationarity intervals. Urban micro-cell site with a regular street grid.

The second wave propagation environment corresponds to a town market square. The size of the square is about 100×100 m. It is partly filled with market stalls. The buildings around the square are of variable size and height. The receiving antenna has been placed approximately 7 m above the square level. The other parameters of the measurement setup as well as the stationarity test procedure parameters are kept the same as in the first propagation scenario described above.

The measured impulse responses and the graph of the mean-square value of the TVFR are demonstrated in Figs. 4 and 5, respectively. The CCDF of the length of the stationarity

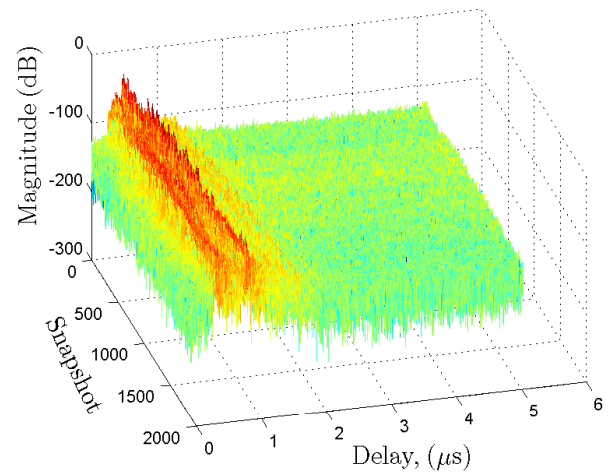


Fig. 4. Magnitude of the impulse response. Town market square.

intervals for SISO, 2×2 MIMO, and 4×4 MIMO channels are depicted in Fig. 6. The average lengths of the identified stationarity intervals decrease from 0.51 s for the SISO channel to 0.25 s for the 2×2 MIMO and 0.14 s for 4×4 MIMO channels, while the corresponding standard deviations

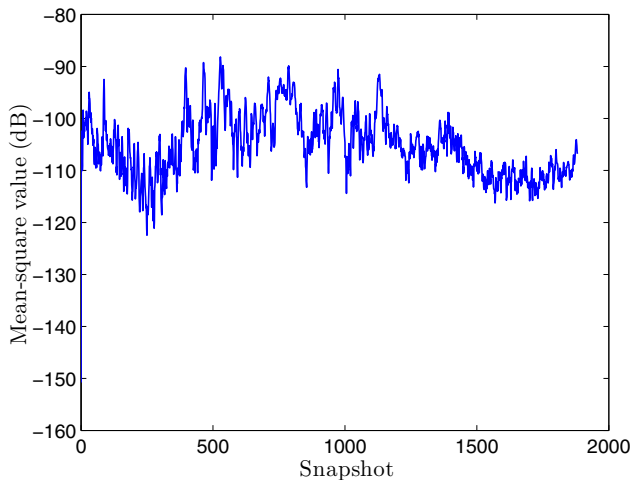


Fig. 5. Mean-square value of the TVFR. Town market square.

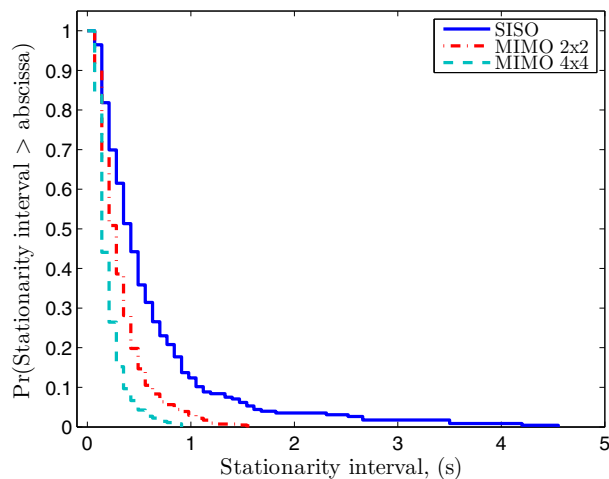


Fig. 6. CCDF of the length of the stationarity intervals. Town market square.

of the stationarity interval lengths are equal to 0.64 s, 0.25 s, and 0.14 s, respectively. Also, the percentage of the identified stationarity intervals longer than or equal to 0.5 s is equal to 36% for the SISO channel, 15% for the 2×2 MIMO, and 4% s for 4×4 MIMO channels. Note that similar to the previously considered propagation environment, the number and the length of the stationarity intervals decrease as the number of antennas at the receiver and transmitter increases.

V. CONCLUSION

In this paper, we propose a stationarity test for wireless communication channels. The test is based on analyzing the delay PSD estimated at two different time instances. If the changes in the estimated delay PSDs are statistically insignificant, the hypothesis that the channel is stationary during the considered time interval is accepted. The proposed stationarity test has been extended to validate the stationarity of real-world MIMO wireless channels.

The analysis of the TVFRs of wireless channels measured in different propagation environments suggests that the length and the number of the channel stationarity intervals are greatly dependent on the number of antennas at the transmitter and the receiver. Generally, the stationarity intervals are longer and occur more often for SISO communication channels compared to MIMO channels. It appears that the measured TVFR becomes more “sensitive” to the changes in the propagation environment as the number of antennas at the transmitter and receiver increases.

ACKNOWLEDGEMENT

The authors would like to thank Telenor R&I, especially, Mr. Per H. Lehne for the kindly provided measurement data and the software for extracting the channel frequency response matrix.

REFERENCES

- [1] P. Bello, “Characterization of randomly time-variant linear channels,” *IEEE Trans. Commun. Syst.*, vol. 11, no. 4, pp. 360–393, Dec. 1963.
- [2] I. G. A. Gehring, M. Steinbauer and M. Grigat, “Empirical channel stationarity in urban environments,” in *Proceedings of the 4th European Personal Mobile Communications Conference (EPMCC '01)*, Vienna, Austria, Feb 2001.
- [3] S. Kay, “A new nonstationarity detector,” *IEEE Trans. Signal Process.*, vol. 56, no. 4, pp. 1440–1451, April 2008.
- [4] R. J. C. Bultitude, G. Brussaard, M. H. A. J. Herben, and T. J. Willink, “Radio channel modelling for terrestrial vehicular mobile applications,” in *Proc. Millenium Conf. Antennas and Propagation*, Davos, Switzerland, Apr. 2000, pp. 1–5.
- [5] J. S. Bendat and A. G. Peirsol, *Random Data: Analysis and Measurement Procedures*, 3rd ed. NY: Wiley-Interscience, 2000.
- [6] R. J. C. Bultitude, “Estimating frequency correlation functions from propagation measurements on fading radio channels: a critical review,” *IEEE J. Sel. Areas Commun.*, vol. 20, no. 6, pp. 1133–1143, Aug. 2002.
- [7] T. J. Willink, “Wide-sense stationarity of mobile MIMO radio channels,” *IEEE Trans. Veh. Technol.*, vol. 57, no. 2, pp. 704–714, March 2008.
- [8] T. S. R. M. B. Priestley, “A test for non-stationarity of time-series,” *J. R. Stat. Soc., Ser. B*, vol. 31, no. 1, pp. 140–149, 1969.
- [9] A. Papoulis and S. U. Pillai, *Probability, Random Variables and Stochastic Processes*, 4th ed. New York: McGraw-Hill, 2002.
- [10] D. B. Percival and A. T. Walden, *Wavelet Methods for Time Series Analysis*. Cambridge University Press, 2006.
- [11] P. Stoica and N. Sandgren, “Smoothed nonparametric spectral estimation via cepstrum thresholding - introduction of a method for smoothed nonparametric spectral estimation,” *IEEE Signal Process. Mag.*, vol. 23, no. 6, pp. 34–45, Nov. 2006.
- [12] V. S. Pugachev, *Probability Theory and Mathematical Statistics for Engineers*. Oxford: Pergamon Press, 1984.
- [13] G. A. F. Seber, *Multivariate Observations*. Wiley, 2004.
- [14] S. L. Marple, *Digital Spectral Analysis with Applications*. NJ: Prentice Hall, 1987.
- [15] M. Ptzold and B. O. Hogstad, “Design and performance of MIMO channel simulators derived from the two-ring scattering model,” in *Proc. 14th IST Mobile & Communications Summit, IST 2005*, Dresden, Germany, June 2005.
- [16] G. D. Durgin, *Space-Time Wireless Channels*. NJ: Prentice Hall, 2003.